Purdue University
Purdue e-Pubs

International Refrigeration and Air Conditioning Conference | School of Mechanical Engineering

2022

A Methodology for Mapping the Performance of Air-to-Air Heat Recovery Ventilators using Laboratory Tests

Jie Ma

W. Travis Horton

James E. Braun

Follow this and additional works at: https://docs.lib.purdue.edu/iracc

Ma, Jie; Horton, W. Travis; and Braun, James E., "A Methodology for Mapping the Performance of Air-to-Air Heat Recovery Ventilators using Laboratory Tests" (2022). *International Refrigeration and Air Conditioning Conference.* Paper 2497.
https://docs.lib.purdue.edu/iracc/2497

This document has been made available through Purdue e-Pubs, a service of the Purdue University Libraries. Please contact epubs@purdue.edu for additional information.
Complete proceedings may be acquired in print and on CD-ROM directly from the Ray W. Herrick Laboratories at https://engineering.purdue.edu/Herrick/Events/orderlit.html

A Methodology for Mapping the Performance of Air-to-Air Heat Recovery Ventilators using Laboratory Tests

Jie MA[1], W. Travis HORTON[1], James E. BRAUN[1]

[1]Ray W. Herrick Laboratories, School of Mechanical Engineering, Purdue University
West Lafayette, 47907-2099, USA
ma319@purdue.edu; wthorton@purdue.edu; jbraun@purdue.edu

ABSTRACT

Air-to-air heat recovery ventilators (HRVs) can significantly reduce heating and cooling loads due to ventilation, especially for applications that have high fresh air requirements. Considering the expected growth in the utilization of HRV equipment due to concerns about virus transmission in buildings, it is important to have accurate methods to characterize their energy performance for use in selecting equipment for a specific building and location. However, current testing and rating standards that are based on laboratory testing do not provide a generalized methodology to fully characterize the energy performance of HRV units. In this paper, a methodology for characterizing the performance of an integrated HRV unit using laboratory testing is presented. The overall HRV unit performance mapping approach involves the use of a model for each component in an HRV unit that is trained using a limited amount of 8 laboratory test data points. The overall approach was validated using 40 experimental data points that were obtained over a wide range of operating conditions. To demonstrate practical use of the resulting HRV performance model that integrates all component models, overall recovered energy and a Coefficient of Performance (COP) were estimated for fixed indoor conditions over a range of outdoor conditions that are typical for cooling and heating dominated climates (Phoenix in AZ and Duluth in MN).

Keywords: Heat Recovery Ventilator, Energy Performance, Energy Saving

1. INTRODUCTION

Air-to-air heat recovery ventilators (HRVs) can effectively reduce energy consumption associated with HVAC systems through transferring heat between the outdoor fresh air steam and the indoor exhaust air stream, which reduces ventilation cooling and heating loads (Zeng et al., 2017). With the proliferation of HRV devices on the market, it is essential to have accurate methods for testing, rating, and evaluating their performance. However, the commonly used standards for HRV unit performance testing and rating, such as AHRI Standard 1060 (2018), CAN/CSA-C439 (2018), and Passive House Institute (PHI) Certification, do not provide sufficient data and appropriate performance metrics to enable the development of accurate models that fully characterize the performance of air-to-air heat and energy recovery ventilators. In these rating standards, the HRV is only tested and assessed under a certain combination of outdoor air drybulb and wetbulb temperatures for heating and cooling, which only covers a small operation condition range relative to the equipment's possible operating conditions. Furthermore, for a traditional ERV/HRV that only contains an energy/heat energy exchanger core, sensible and latent effectivenesses are typically utilized as performance indicators to characterize the heat exchanger's energy recovery effectiveness. However, innovative ERV units contain additional integrated components, such as an economizer, preheater, supply fan, and exhaust fan. The effectivenesses for the energy exchanger core cannot fully characterize the overall unit performance for these ERV types.

Several studies utilizing field testing have been conducted to better comprehend and characterize the overall performance of specific HRVs (Liu et al., 2010; Zhang and Fung 2014). However, there are no general equipment performance testing approaches to rate and certify equipment or methods to obtain a performance model that can be integrated into building simulation software. In order to evaluate the energy performance of particular equipment under a wide range of environmental conditions using field data, it would be necessary to install the equipment in

different climate zones and to then collect data during different seasons. Furthermore, the process would need to be repeated for different equipment to be evaluated. However, it is much more practical and cost effective to fully characterize equipment performance over a wide range of conditions using a laboratory test approach.

In this study, a methodology is proposed for testing and mapping the performance of HRV equipment utilizing laboratory environmental chambers. The proposed method allows overall energy assessments under a variety of indoor and outdoor conditions and employs a model in which each component of an HRV unit is trained using a limited number of 8 laboratory test data points. The modeling approach is validated with 40 experimental data points spanning a wide range of operating situations. It is demonstrated that the developed overall unit model can be used to estimate the overall recovered energy and a Coefficient of Performance (COP) in both cooling and heating-dominated regions (e.g., Phoenix in AZ and Duluth in MN).

2. LABORATORY EXPERIMENT

The HRV unit was installed in an environmental chamber that was controlled to simulate outdoor conditions. As depicted in Figure 1, the experimental setup consists of two separate open air circuits: 1) a fresh air and supply air circuit and 2) a return air and exhaust air circuit. During each test, the following parameters were gathered for future model development: (1) dry-bulb and dew-point temperatures at OA, RA inlets and at SA, EA outlets; (2) air volume flow rate of the two air circuits (OA-SA circuit and RA-EA circuit); (3) power input for the supply and exhaust fans ($PW_{\text{fan,SA}}$, $PW_{\text{fan,EA}}$) as well as power input for the entire unit (PW_{unit}).

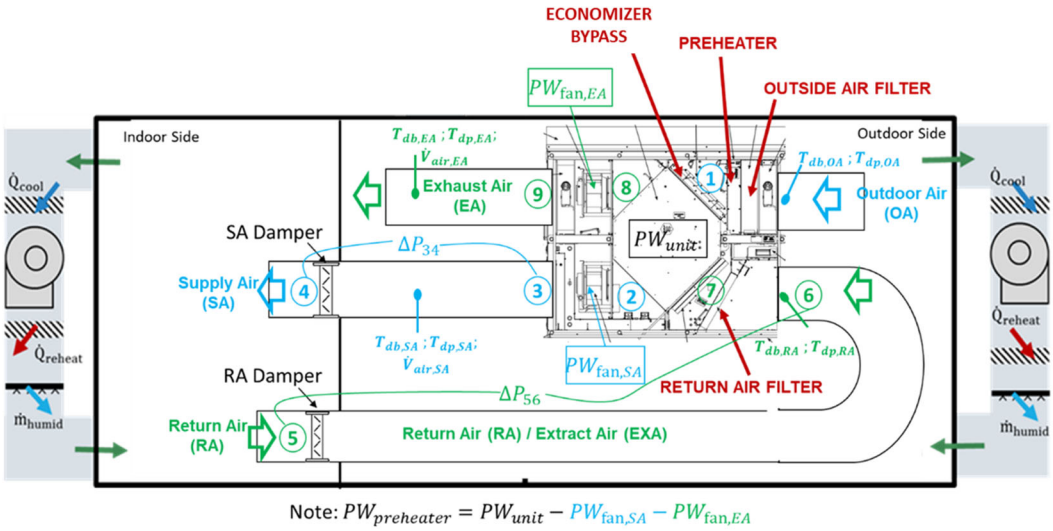

Figure 1: ERV test ductwork configuration modification

The testing matrix for HRV performance rating is listed in Table 1, which takes into account both cooling and heating air handling processes. In addition, the air flow rates in the two air circuits were balanced and varied from the lowest value of 180 CFM to the highest value of 1020 CFM with increments of 180 CFM. In those tests, 48 data points were collected and used for HRV performance mapping and model validation. Each test was operated until stabilized conditions were reached, then data was sampled at 1s intervals for a period of 30 minutes.

Table 1: Testing matrix for HRV performance rating

Indoor Conditions (Dry-bulb temperature, Relative humidity)	**Outdoor Conditions** (Dry-bulb temperature, Relative humidity)
75°F,50%	113°F, 16%; 104°F, 21%; 95°F, 26%; 86°F, 36%; 65°F, 70%
75°F, 20%	56°F; 70%; 47°F; 70%; 38°F; 70%

To test the energy balance of the heat exchanger core, heat exchange rates in the two air circuits were calculated. The heat exchange rate is derived from measurements of airflow and the entering and exiting air temperatures using energy balances as

$$\dot{Q}_{core,SA} = \dot{m}_{SA} c_p (T_{SA} - T_{OA}) - PW_{fan,SA} - PW_{preheater}$$
$$\dot{Q}_{core,EA} = \dot{m}_{EA} c_p (T_{EA} - T_{RA}) - PW_{fan,EA} \quad (1)$$

where T is dry-bulb temperature. The subscripts OA, RA represent outdoor air and return air entering the unit, respectively; SA and EA represent supply air and exhaust air leaving the unit, respectively. $\dot{m}$ is air mass flow rate. c_p is the corresponding air specific capacity. PW is the power input. When outdoor air is cooled, the heat exchange rate in the supply air circuit is negative, while it is positive in the exhaust air circuit. When outdoor air is heated, the heat exchange rate in the supply air circuit is positive, whereas it is negative in the exhaust air circuit.

In addition, since two fans were positioned downstream of the heat exchanger core but upstream of the thermocouple grids used to measure drybulb temperature, heat production from the two fans was also considered in the energy balance n. When the preheater was activated, the preheater's power input was accounted for in the energy balance.

Uncertainty analysis was conducted based on JCGM GUM 100-2008 (JCGM, 2008), which states that the combined uncertainty of outputs is obtained by combining the standard uncertainties of input estimates. To analyze the energy balance, the sensible energy recovery rates in the heat exchanger core for the outdoor air circuit and the return air circuit were computed. As depicted in Figure 2, all obtained experimental data revealed acceptable sensible energy balance accuracy (error bands are within $\pm 10\%$).

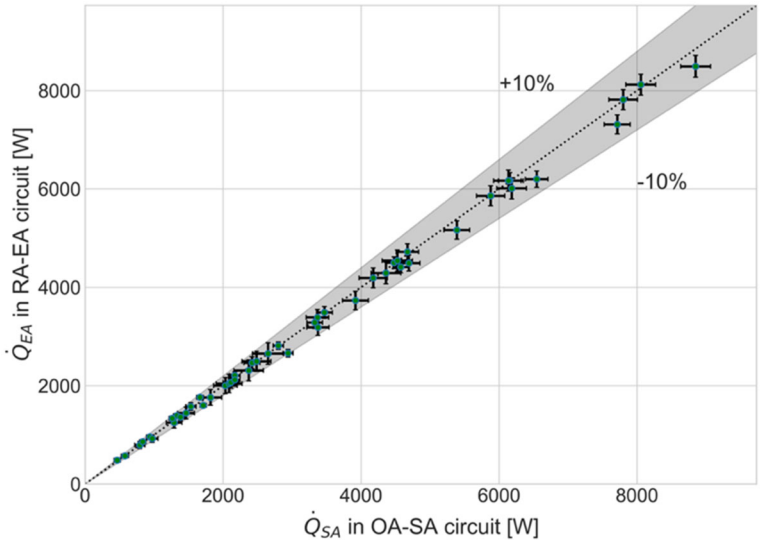

Figure 2: Comparison of absolute values of sensible core energy recovery rates for two air circuits (energy balance)

3. PERFORMANCE MAPPING DEVELOPMENT

This section describes the development of the method used for predicting the overall HRV unit's performance in which physical-based models for the unit's main components are combined.

3.1 Heat exchanger model

Sensible effectiveness is a rating metric to evaluate the performance of an HRV energy exchanger core:

$$\varepsilon_{sen} = \frac{\dot{m}_{SA} c_p (T_{SA} - T_{OA}) - PW_{fan,SA} - PW_{preheater}}{min\,(\dot{m}_{OA} c_p, \dot{m}_{RA} c_p)(T_{RA} - T_{OA})} \quad (2)$$

The outdoor air temperature and air flow rate were plotted against sensible core recovery efficiency to investigate the effects of inlet air temperature and air flow rate on the heat exchanger core's heat recovery performance. As shown in Figure 3 (a), the sensible recovery effectiveness of the core increased as the outdoor air temperature rose for both heating and cooling energy recovery, but there was a dramatic difference in effectiveness between heating mode conditions (below 65°F outdoor air temperature) and cooling model conditions (above 85°F outdoor air temperature). It is shown in Figure 3 (b) that the sensible recovery effectiveness of the core decreased slightly as the supply air flow rate increased for all outdoor air temperature cases studied in this work.

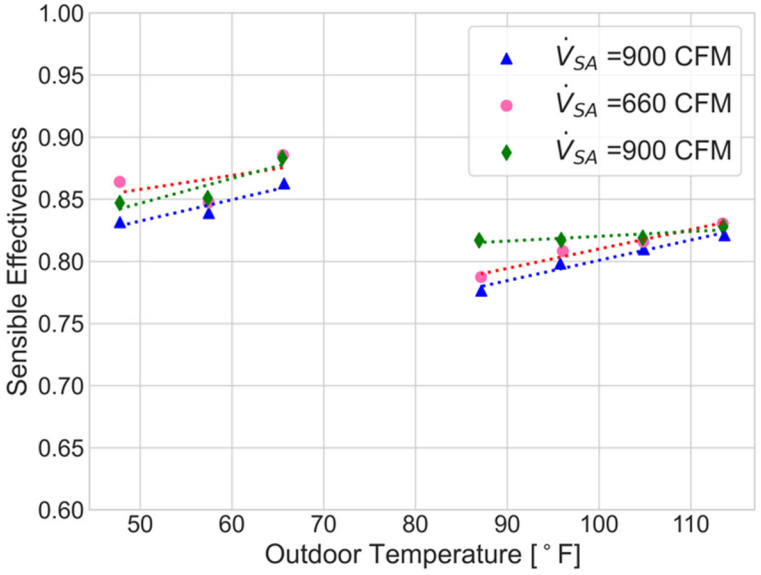

(a)

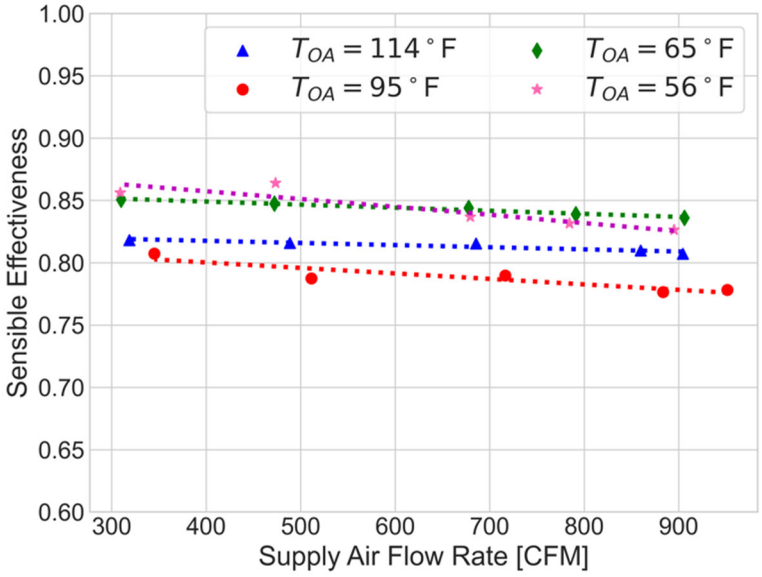

(b)

Figure 3: Effect of operating conditions on sensible core recovery effectiveness of HRV unit: (a) outdoor air temperature, (b) supply air flow rate

In developing a mapping approach, relations for sensible energy recovery effectiveness of a crossflow heat exchanger were employed that are based on the *ε-NTU* method (Qiu et al., 2019; Noie, 2006):

$$\varepsilon_{sen,core} = 1 - \exp\left\{\left(\frac{m_{min}}{m_{max}}\right) Ntu^{0.22} \times \left[\exp\left(-\frac{m_{min}}{m_{max}}\right) Ntu^{0.78}\right] - 1\right\} \quad (3)$$

$$Ntu = \frac{hA}{(mc_p)_{min}} \quad (4)$$

$$hA = \mathrm{a}_0 + \mathrm{a}_1 \mathrm{V} + a_2(T_{OA} - T_{RA}) \quad (5)$$

where m_{min} and m_{max} represent the smaller and larger air flow rates between the supply and exhaust air circuits, respectively. *hA* is an overall conductance for sensible heat transfer which is assumed to be a linear function of airflow rate and temperature difference between outdoor air and return air, according to the sensitivity analysis in Figure 3. The heat exchanger effectiveness map is generated separately for cooling and heating season operation. For the cooling season, the training data set contained 4 data points, which correspond to test data at outdoor temperatures of 95°F and 113°F, each of which is paired with air flow rates of 900 CFM and 300 CFM. For the heating season, the training data set contains four data points with outdoor temperatures of 56°F and 47°F, along with air flow rates of 900 CFM and 300 CFM. Overall, 8 data points were utilized to train the model of the heat exchanger, whereas 40 data points were used to validate the model.

3.2 Fan and Preheater Model

The supply fan and exhaust fan located downstream of the heat exchanger are the main components that provide air flow. In this study, a simple polynomial-based curve-fit model is used to describe the relation between volume flow rate and fan power input.

In frost-protection mode, the preheater is activated and consumes additional energy to ensure that the exhaust air leaving the exchanger ($T_{\mathrm{EA,core}}$) is no lower than a setpoint temperature that is well above freezing. The control sequence of the tested HRV unit under frost-protection mode is as follows:

1) When the required instantaneous preheater power input is lower than its nominal value, the preheater is cycled on and off based on the temperature difference between the exhaust air leaving the exchanger ($T_{\mathrm{EA,core}}$) and its setpoint. To characterize the quasi-steady behavior over a complete on/off cycle, the average preheater power input is assumed to be equal to its nominal value multiplied by the ratio of run-time to cycle time.
2) When the required instantaneous preheater power input is larger than its nominal value, the preheater power input is maintained at its nominal value, and the temperature of exhaust air gradually drops as the outdoor temperature decreases.
3) When the preheater is operating at its maximum power input but the measured temperature of exhaust air leaving the heat exchanger is still below a pre-set minimum limit (i.e., $T_{EA,core,preheater=max} \leq T_{EA,min}$), the outdoor air fully bypasses the heat exchanger, resulting in no energy being recovered in the heat core, and the preheater is turned off.

For situations (1) and (2), the temperature of the outdoor air leaving the preheater and entering the energy exchanger ($T_{OA,core,in}$) is obtained by

$$T_{OA,core,in} = \frac{PW_{preheater}}{\dot{m}_{SA} c_p} + T_{OA} \quad (6)$$

where $PW_{preheater}$ is the preheater's power input. In the frost-protection mode, the heat exchanger's operation is not interrupted and the heat exchanger effectiveness is equal to the effectiveness without frosting. Accordingly, the supply air leaving the heat exchanger is computed depending on the heat exchanger's characteristics as

$$T_{SA,core} = T_{OA,core,in} - \varepsilon_{sen,core}\left(\frac{m_{min}}{m_{SA}}\right)(T_{OA} - T_{RA}) \quad (7)$$

3.3 Economizer Model

In order to provide free cooling or prevent overheating, the HRV unit's built-in economizer modulates the economizer damper to bypass outdoor air across the heat exchanger. In this work, the control strategy in conjunction with the economizer bypass operation is a dry-bulb temperature-based control method, where the economizer damper is modulated depending on the measured supply air temperature, return air temperature (T_{RA}) and supply air setpoint ($T_{SA,sp}$):

1) $T_{SA,sp} \leq T_{OA} \leq T_{RA}$: the outdoor air completely bypasses the heat exchanger, and there is no energy recovery in the heat exchanger. At this point, the temperature of the supply air leaving the heat exchanger and entering the supply fan is equivalent to the outdoor air temperature ($T_{SA,core} = T_{OA}$). The supply air setpoint is

consistent with a building balance point temperature which is defined as the outdoor temperature where no mechanical cooling or heating is required to maintain the indoor temperature because of internal gains.

2) $T_{OA} < T_{SA,sp}$ *or* $T_{OA} > T_{RA}$: the outdoor temperature falls below supply air setpoint or rises above the indoor temperature, the economizer damper is closed and the outdoor air completely flows through the heat exchanger.

3.4 Overall Unit Model

By combining all component models with the unit's in-built control logic, the overall HRV unit performance can be predicted. First, the boundary conditions, including indoor and outdoor air temperature, as well as air flow rate in the two air circuits are specified as inputs. The sensible recovery effectiveness for the heat exchanger core is obtained at the given air flow rates and boundary conditions using the sensible heat exchanger $\varepsilon - Ntu$ modeling approach (expressed in Eq.(3) to Eq.(5)), with the goal of determining the temperature of the supply air and exhaust air leaving the energy exchanger when the outdoor air flows completely through the heat exchanger without opening the economizer damper or activating the preheater.

$$T_{SA,core} = T_{OA} - \varepsilon_{sen,core}\left(\frac{m_{min}}{m_{SA}}\right)(T_{OA} - T_{RA}) \tag{8}$$

$$T_{EA,core} = T_{RA} - \varepsilon_{sen,core}\left(\frac{m_{min}}{m_{EA}}\right)(T_{OA} - T_{RA}) \tag{9}$$

The HRV unit's embedded control logic for the operation of each main component is presented in Figure 4:

1) When the temperature of the outdoor air is higher than the temperature of the return air, the outdoor air flows through the heat exchanger. The temperature of supply air exiting the heat exchanger is calculated by Eq.(8).
2) When the outdoor air temperature is lower than the return air temperature but higher than the supply air setpoint, the outdoor air completely bypasses the heat exchanger. The temperature of supply air leaving the heat exchanger core is equal to the temperature of outdoor air, and no energy is recovered in heat exchanger.
3) When the outdoor air temperature is lower than the supply air setpoint, the preheater activation decision procedure is initiated. The supply air leaving the heat exchanger is recalculated using the model outlined in Section 3.2.

The overall energy recovery rate for the integrated unit depends on the energy recovered in the heat exchanger and the heat generated by the supply fan and preheater, which is calculated as

$$\dot{Q}_{HRV} = m_{SA}c_p\left(T_{SA,core} - T_{OA}\right) + PW_{fan} + PW_{preheater} \tag{10}$$

The total electric power input for the HRV unit is the sum of the power input for the two fans and the preheater. An energy performance indicator for an HRV unit, i.e., coefficient of performance (COP), is defined as the ratio of overall recovered energy to total electric energy consumed:

$$COP = \frac{\left|\dot{Q}_{HRV}\right|}{PW_{total}} \tag{11}$$

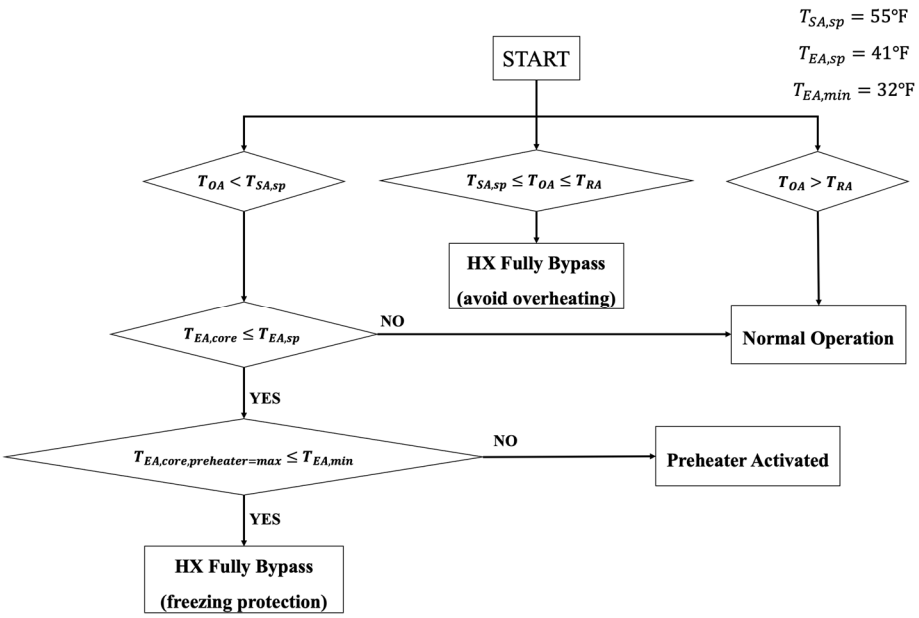

Figure 4. Flow chart of overall unit performance model

Figure 5 compares the overall energy recovery rates for the tested HRV unit (which was obtained from the experimental results) and overall model predictions. The overall $MAPE$ was 8.0% and the R^2 was 98.8%. Figure 6 shows a slightly lower MAPE value of 7.1% and a lower R^2 of 98.3% when comparing COPs between experimental findings and model-predicted values. The results indicate that the majority of data points fall within an error margin of 15%. Taking into account the large range of the tested experimental conditions, this agreement is considered satisfactory.

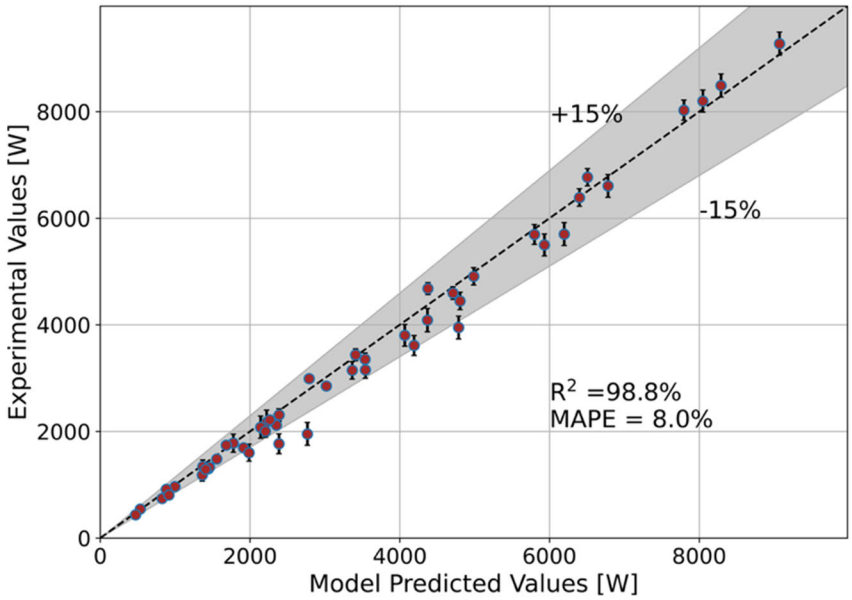

Figure 5. Comparison of overall experimental and model predicted energy recovery rates

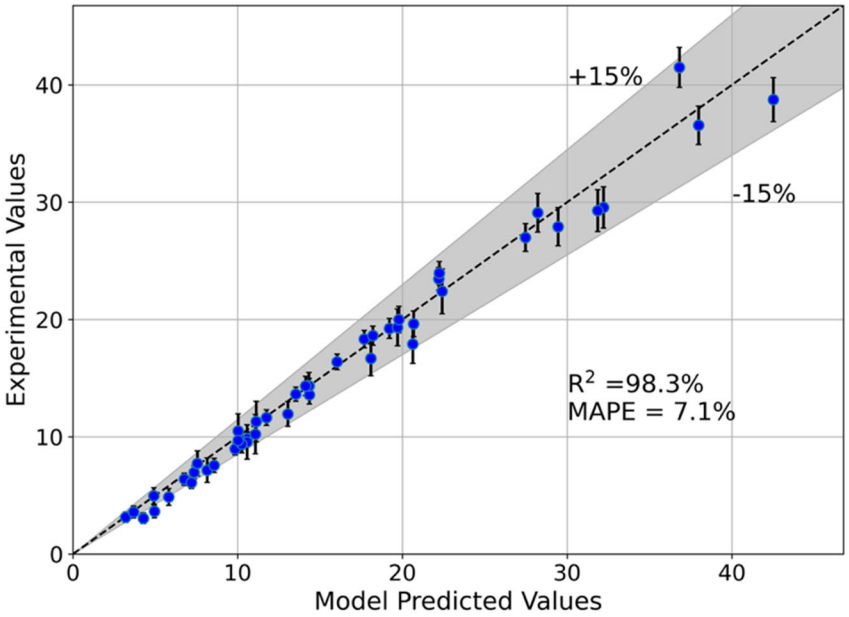

Figure 6. Comparison of experimental and model predicted COPs

3.5 Overall Unit Model Application

The overall performance model for an HRV unit can be applied to predict overall recovered energy and equipment COP at any operating condition. In this study, the performance of the HRV unit was estimated under fixed indoor conditions, as indicated in

Table 2, and over a range of outdoor conditions that are typical for cooling and heating dominated climates (Phoenix in AZ and Duluth in MN) and that could be integrated with a simplified bin method. In considering application within the bin method, the outdoor temperatures for the two climates were sorted into discrete bins with a fixed temperature bin interval of 5°F . Each bin records the number of hours in which the outdoor temperature falls within its associated temperature interval. The recovered energy and power consumption for each bin ($Q_{HRV,j}$ and $E_{total,j}$) are determined by multiplying the recovered energy rate and total power input at the temperature represented for each bin by the number of occurrence hours associated with that bin, respectively. The recovered energy is negative when supply air is cooled and is positive when incoming supply air is heated by recovering heat from outgoing exhaust air.

The equipment COP for each bin is calculated as follow.

$$COP_j = \frac{|Q_{HRV,j}|}{E_{total,j}} \tag{12}$$

Table 2: Indoor conditions for bin-method calculation

Cooling Season		Heating Season	
Dry-bulb temperature	Wet-bulb temperature	Dry-bulb temperature	Wet-bulb temperature
75°F	63°F	70°F	56°F

Figure 7 demonstrates model prediction results for overall recovered energy and HRV equipment COP for the Phoenix climate across a range of ventilation flow rates, when the outdoor air temperature exceeds the supply air setpoint for economizer mode. At an outdoor temperature between 55°F and 75°F, both recovered energy and equipment COP were close to zero because the outdoor air bypassed the heat exchanger core entirely in economizer mode. Assuming a constant ventilation flow, the overall recovered energy and equipment COP increased as the outdoor dry-bulb temperature exceeded 77°F and rose with the increase in outdoor air temperature. This is because the energy recovery in the unit grew as the indoor-to-outdoor temperature differential increased, yet the input power remained constant due to the fixed air flow rate. Based on the aforementioned findings, it can be concluded that, the

HRV should be activated when the outdoor air temperature is above 82°F in order to recover energy effectively in a cooling domain climate. In the cooling season, the more time the outdoor air temperature exceeds 82°F, the greater the HRV unit's potential benefits.

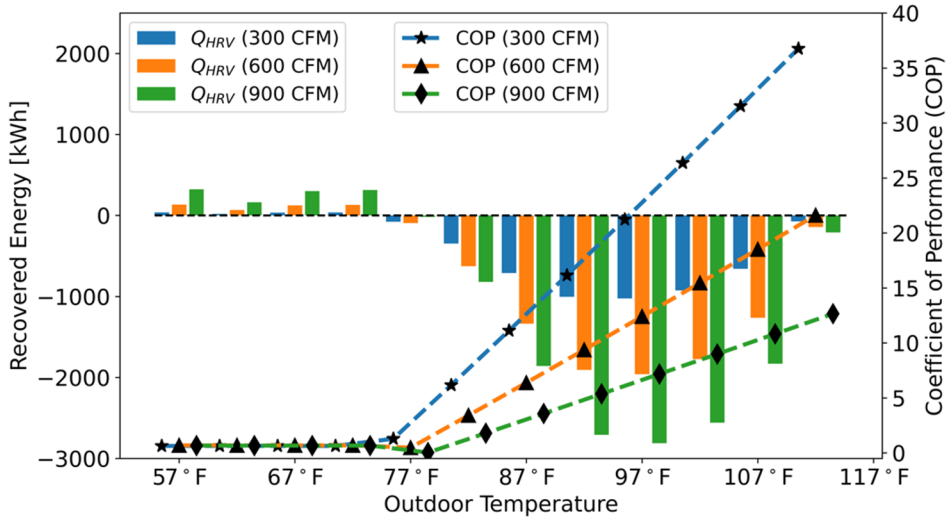

Figure 7: Recovered energy and equipment COP of HRV for each temperature bin of cooling season in Phoenix

Figure 8 represents model prediction results for overall recovered energy with an HRV in Duluth for a variety of ventilation flow rates, when the outdoor air temperature is below the supply air setpoint for economizer mode. As the outdoor temperature fell below the supply air setpoint for economizer mode (which is 55°F), the outdoor air completely flowed through the heat exchanger core and the indoor-outdoor temperature difference increased, which resulted in an increase in the unit's overall recovery energy and COP. At outdoor temperatures below about 37°F, the COP decreased with decreasing temperature because the preheater was activated for frost protection, resulting in a significant rise in the unit's power input. In this case, the increase of power input with decreasing outdoor temperature exceeded the increase in the unit's recovered energy. When the outdoor temperature fell below 2°F for a 900 CFM supply air flow rate or below -8°F for a 600 CFM supply air flow rate, the supply air completely bypassed the heat exchanger for freeze protection, bringing the overall recovered energy and equipment COP close to zero. In this situation, the HRV unit is only providing ventilation air and not heat recovery. As a result of the control logic and features employed with this HRV unit, in heating seasons, the best overall heat recovery performance (highest COP) occurs between outdoor temperatures of 37°F and 55°F.

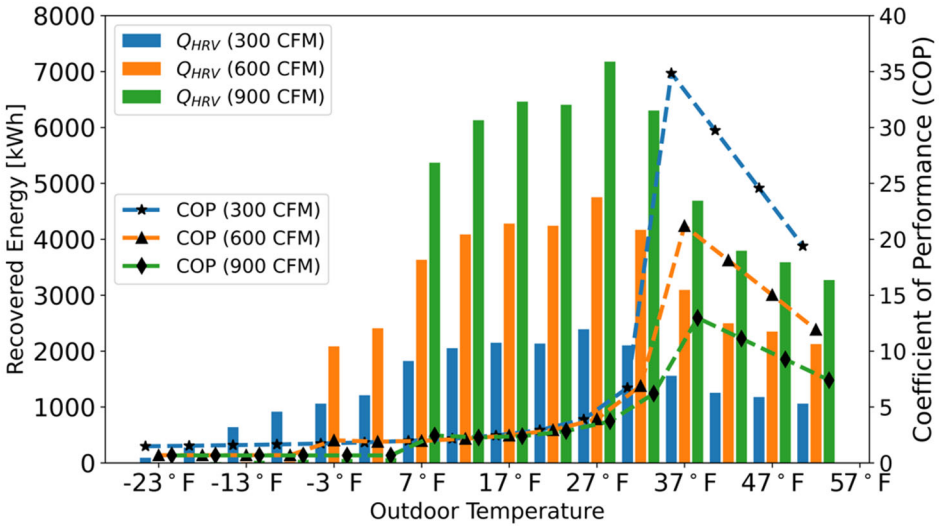

Figure 8: Recovered energy and equipment COP of HRV for each temperature bin of heating season in Duluth

4. Summary

In this work, methodologies for testing and mapping the performance of HRV equipment in laboratory environmental chambers were developed, allowing overall energy assessments for a wide range of outdoor conditions. The HRV unit model was trained with a small data set consisting of only 8 data points and was validated with 40 experimental data points encompassing a wide range of outdoor temperature. Using the developed HRV model, the performance of the tested HRV unit in various equipment operation modes (normal mode with fully outdoor air recovered, frost-protection and economizing bypass) can be characterized. Good agreement between the experimental data and the model-predicted values was obtained with an $MAPE$ of 7.7% and a R^2 of 98.8% for energy recovery rate and a $MAPE$ of 7.1% and a R^2 of 98.3% for equipment COP. This HRV model can be used to evaluate the performance of HRV equipment under any given set of indoor and outdoor conditions. As an example, the overall recovered energy and equipment COP were predicted under outdoor conditions representative of cooling and heating-dominated regions, respectively.

In the future, the modeling methodology will be applied to test data for other HRV/ERV equipment to investigate the potential for generalization and rating standardization.

Nomenclature

$\dot{m}$	mass flow rate $[kg \cdot h^{-1}]$	$\dot{Q}$	recovered energy rate $[W]$
c_p	specific capacity $[J{\cdot}kg^{-1}{\cdot}K^{-1}]$	PW	power input $[W]$
T	dry-bulb temperature [°F]	$Q_{HRV,j}$	recovered energy for j bin $[kWh]$
ε_{sen}	Sensible effectiveness [-]	$E_{total,j}$	total energy consumption for j bin $[kWh]$

Subscript

OA	outdoor air	SA	supply air
RA	return air	EA	exhaust air
COP	Coefficient of Performance		

References

AHRI Standard 1060 (SI)-2018, Performance Rating Air-to-Air Exchangers for Energy Recovery Ventilation Equipment, 2018, Air-Conditioning, Heating, and Refrigeration Institute, 2311 Wilson Boulevard, Suite 500, Arlington, VA 22201, U.S.A.

CAN/CSA-C439-18. Standard laboratory methods of test for rating the performance of heat/energy-recovery ventilators. January 2018.

JCGM, 2008. Evaluation of measurement data — Guide to the expression of uncertainty in measurement. International Organization for Standardization Geneva ISBN 50, 134.

Liu, J, Li, W., Liu, J, Wang, B., 2010. Efficiency of energy recovery ventilator with various weathers and its energy saving performance in a residential apartment. Energy and Buildings 42, 43–49. https://doi.org/10.1016/j.enbuild.2009.07.009

Noie, S. H. (2006). Investigation of thermal performance of an air-to-air thermosyphon heat exchanger using ε-NTU method. Applied Thermal Engineering, 26(5-6), 559-567.

Qiu, S., Li, S., Wang, F., Wen, Y., Li, Zhenhai, Li, Zhengwei, Guo, J., 2019. An energy exchange efficiency prediction approach based on multivariate polynomial regression for membrane-based air-to-air energy recovery ventilator core. Building and Environment 149, 490–500. https://doi.org/10.1016/j.buildenv.2018.12.052

Zeng, C., Liu, S., Shukla, A., 2017. A review on the air-to-air heat and mass exchanger technologies for building applications. Renewable and Sustainable Energy Reviews 75, 753–774. https://doi.org/10.1016/j.rser.2016.11.052

Zhang, J., Fung, A.S., 2014. Experimental study and analysis of an energy recovery ventilator and the impacts of defrost cycle. Energy and Buildings 87, 265–271. https://doi.org/10.1016/j.enbuild.2014.11.050